Available online at www.sciencedirect.com

SciVerse ScienceDirect

Ceramics International 39 (2013) 1677–1681

CERAMICS INTERNATIONAL

www.elsevier.com/locate/ceramint

Improving ferroelectric and piezoelectric properties of $PbFe_{1/4}Sc_{1/4}Nb_{1/2}O_3$ ceramics by oxide doping prepared via a B-site oxide mixing route

Bijun Fang[a,*], Meijuan Zhu[a], Jianning Ding[a,b], Yuejin Shan[c], Hideo Imoto[c]

[a]School of Materials Science and Engineering, Changzhou University, Changzhou, Jiangsu 213164, China
[b]School of Material Science and Engineering, Jiangsu University, Zhenjiang, Jiangsu 212013, China
[c]Department of Applied Chemistry, Faculty of Engineering, Utsunomiya University, 7-1-2 Yoto, Utsunomiya 321–8585, Japan

Received 28 June 2012; received in revised form 23 July 2012; accepted 4 August 2012
Available online 11 August 2012

Abstract

Oxide-doped $PbFe_{1/4}Sc_{1/4}Nb_{1/2}O_3$ (PFSN) ceramics were prepared by the conventional ceramic processing via a B-site oxide mixing route. The oxide-doped PFSN ceramics exhibit pure rhombohedral perovskite structure and high relative density. Due to the MnO_2 and Li_2CO_3 doping, the synthesized ceramics exhibit improved dielectric property, and excellent ferroelectric and piezoelectric properties, which can be attributed to a charge compensation mechanism where donor defects are generated by different ionization paths. The values of remnant polarization P_r, electromechanical coupling coefficient K_p and piezoelectric constant d_{33} of the MnO_2- and Li_2CO_3-doped PFSN ceramics are 16.35 μC/cm^2, 0.232 and 112.7 pC/N, and 29.22 μC/cm^2, 0.241 and 112.5 pC/N, respectively. Therefore, oxide doping is an efficient method to improve dielectric, ferroelectric and piezoelectric properties of the PFSN-based ferroelectric ceramics.

Keywords: C. Ferroelectric property; C. Piezoelectric property; Crystal structure; $PbFe_{1/4}Sc_{1/4}Nb_{1/2}O_3$-based ceramics

1. Introduction

Relaxor ferroelectric ceramics exhibit excellent electrical properties, which make them promising applications in multilayer capacitor and related versatile application fields [1–5]. 1:1-type lead-based complex perovskite relaxors $Pb(Fe_{1/2}Nb_{1/2})O_3$ (PFN) and $Pb(Sc_{1/2}Nb_{1/2})O_3$ (PSN) attract our research attention since PFN and PSN exhibit rhombohedral perovskite structure and complete solid solution $(1-x)Pb(Fe_{1/2}Nb_{1/2})O_3$-$xPb(Sc_{1/2}Nb_{1/2})O_3$ (PFN–PSN) can form in the whole composition range [6–9].

The nature of relaxor behavior has attracted enormous fundamental investigations. Usually, the relaxor behavior is attributed to the polar clusters and/or the nanoscopic inhomogeneity induced by the random occupation of the crystallographic equivalent positions by different cations [10,11]. Such structural character produces short-range occupational ordering and engineered domain configuration, which prevents the complete development of long-range ferroelectric ordering, destroys the normal ferroelectric phase transition and makes the physical properties of the relaxor ferroelectrics similar to those of the disordered ferromagnetic materials [12,13]. However, the understanding of the relaxor properties is not yet satisfactory [14,15].

In this paper, the composition $PbFe_{1/4}Sc_{1/4}Nb_{1/2}O_3$ (PFSN) is adopted for further optimization since PFSN crystallizes into a pseudo-cubic structure around room temperature and exhibits relatively large dielectric constant, low sintering temperature, and relaxor behavior. Since the iron- and scandium-containing ferroelectric ceramics tend to exhibit large dielectric loss and strong dielectric frequency dispersion, the pure PFSN ceramics exhibit deteriorated ferroelectric and piezoelectric properties. In views of crystal chemistry and materials engineering, the differences of ionic size, atomic weight, electric negative, and/or charge are produced by cation substitution on the crystallographic equivalent A-site and/or B-site of the perovskite structure [16,17], which provides straightforward experimental method for systematically tuning electrical properties of piezoelectric

*Corresponding author. Tel./fax: +86 519 86330095.
E-mail addresses: fangbj@sohu.com, fangbj@cczu.edu.cn (B. Fang).

0272-8842/$ - see front matter
http://dx.doi.org/10.1016/j.ceramint.2012.08.010

materials [18]. Therefore, chemical doping MnO_2 and Li_2CO_3 are used to improve electrical properties of the Fe- and Sc-containing ferroelectric ceramics. Through adjustment of the composition of the solid solution, defect structure, spontaneous polarization, electrostatic interactions, and ordering degree of the perovskite structure may be influenced, which provides the possibility to tailor electrical properties of PFN–PSN [7,16,17,19].

2. Experimental procedure

The oxide-doped PFSN ceramics were prepared by the conventional solid-state reaction method via a B-site oxide mixing route, in which all oxides of the B-site of the perovskite structure were pre-calcined simultaneously instead of preparing different wolframite precursors separately [20]. High-purity oxides and carbonate, PbO ($>99.9\%$), Fe_2O_3 ($>99.99\%$), Sc_2O_3 ($>99.9\%$), Nb_2O_5 ($>99.9\%$), MnO_2 ($>99.95\%$), and Li_2CO_3 ($>99.9\%$), were used as raw materials. To maintain stoichiometry the raw materials were dried before weighing and the synthesized B-site precursors were weighed and introduced into the batch weighing. The well-mixed stoichiometric B-site oxides, Fe_2O_3, Sc_2O_3 and Nb_2O_5, were pre-calcined at 1200 °C for 3 h. After crushing and grinding, stoichiometric PbO and 0.25 wt% oxide dopants were added to the synthesized B-site precursors, and the mixed powders were calcined at 900 °C for 2 h. X-ray diffraction measurement (XRD, Rigaku RINT-2200 VS diffractometer) confirmed that the calcined powders exhibit pure perovskite structure. Then the calcined powders were isostatically pressed into pellets at a pressure of 400 kgf/cm^2 with the addition of 1 wt% polyvinyl alcohol (PVA) and sintered at 1160 °C for 2 h. The green pellets were buried under a mixture of raw materials with equal weight and same composition of the pellets in a covered alumina crucible to minimize the evaporation of lead during sintering.

The sintered oxide-doped PFSN ceramics were ground and polished to obtain flat and parallel surfaces. XRD measurement confirmed that the synthesized ceramics maintain perovskite structure during the sintering process. The elemental distribution of the sintered ceramics was measured by an Energy dispersive X-ray fluorescence elemental analyzer (XRFEA, RoHs SEA-2010). For electrical properties characterization, silver paste was coated on both surfaces of the well-polished ceramics and fired at 650 °C for 15 min to provide robust electrodes. Dielectric property under direct current (DC) bias voltage was measured by a Turnkey broadband dielectric spectrometers Concept 42 (Novocontrol Technologies GmbH & Co. KG, Germany). Polarization–electric field (P–E) hysteresis loop was characterized by a Radiant Precision Premier LC ferroelectric material test system (Radiant Technologies Inc., USA), in which a Sigma Model M10 chamber was attached to measure the P-E loop upon heating. The Sigma Model M10 chamber was controlled by a Sigma Systems Model C4 programmable temperature controller, which can measure the thermal range −100 to 200 °C (Sigma Systems Corporation, USA). During the P–E hysteresis loop measurement, the ceramics were immersed in silicon oil to prevent arching. For piezoelectric property measurement, the oxide-doped PFSN ceramics were poled under an electric field of 2 kV/mm at 80 °C for 15 min in silicon oil and then slowly cooled down to room temperature with maintaining half of the applied electric field. Piezoelectric property was measured by a ZJ-6A Berlincourt-type quasi-static d_{33}/d_{31} meter (Institute of Acoustics, Chinese Academy of Sciences, Beijing, China). Detailed performance measurement procedures were described elsewhere [21].

3. Results and discussion

In previous work [22], we reported that the 1160 °C sintered oxide-doped PFSN ceramics exhibit pure rhombohedral perovskite structure, densified microstructure morphology, high relative density and improved dielectric property, which are especially favorable for improving ferroelectric and piezoelectric properties of the PFSN-based ceramics.

The elemental distribution is important for understanding of the effects of oxide doping on the electrical properties of the PFSN-based ceramics. Fig. 1 shows XRFEA spectra of the MnO_2-doped PFSN ceramics. The average values of elemental contents based on the XRFEA measurement are shown in the figure. The elemental contents at different sites exhibit slight difference, especially for Mn^{2+}, indicating that the preparation of homogeneous ceramics is difficult, which will affect local crystal structure and electrical properties of the sintered ceramics. However, the variation of elemental concentration is not apparent. Therefore, the nominal composition can be used to represent the real composition of the oxide-doped PFSN ceramics within the detection sensitivity of XRFEA.

The shape of P–E ferroelectric hysteresis loops is influenced greatly by electric field strength and frequency. Fig. 2

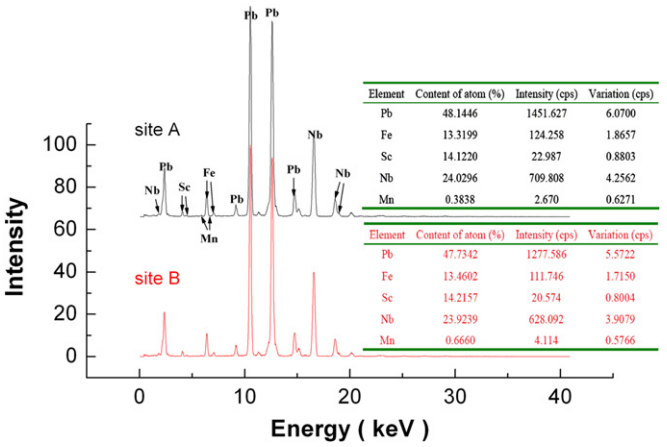

Element	Content of atom (%)	Intensity (cps)	Variation (cps)
Pb	48.1446	1451.627	6.0700
Fe	13.3199	124.258	1.8657
Sc	14.1220	22.987	0.8803
Nb	24.0296	709.808	4.2562
Mn	0.3838	2.670	0.6271

Element	Content of atom (%)	Intensity (cps)	Variation (cps)
Pb	47.7342	1277.586	5.5722
Fe	13.4602	111.746	1.7150
Sc	14.2157	20.574	0.8004
Nb	23.9239	628.092	3.9079
Mn	0.6660	4.114	0.5766

Fig. 1. Energy dispersive X-ray fluorescence spectra of the MnO_2-doped PFSN ceramics measured at different sites. Inset of the figure shows the average values of elemental content.

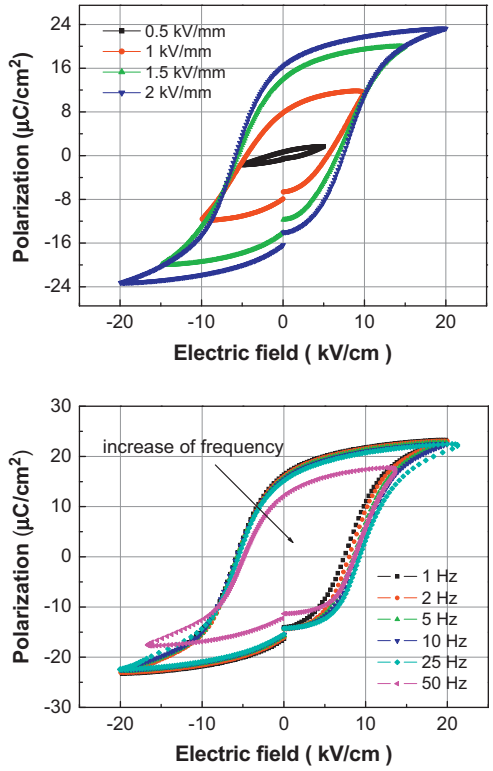

Fig. 2. Room-temperature P–E hysteresis loops of the MnO_2-doped PFSN ceramics measured at different electric fields and frequencies.

shows P–E hysteresis loops of the MnO_2-doped PFSN ceramics. For ferroelectric ceramics, large electric field can afford enough energy for ferroelectric domains to switch and align along the direction of the external electric field. Therefore, at 0.5 kV/mm, a nearly linear P–E relationship is observed, and at 2 kV/mm, a saturate P–E loop is fully developed, correlating with the activation energy needed for the rotation of the ferroelectric domains. For all the electric field measured, the obtained P–E hysteresis loops are rather symmetric and no apparent pinning effect appears. Low frequency is favorable for different polarization mechanisms to follow up the change of the external electric field. Between 1–25 Hz, the P–E hysteresis loops are fully developed, saturated and symmetric with almost the same values of remnant polarization P_r and coercive field E_C. At 50 Hz, the P–E hysteresis loop exhibits apparent asymmetry, indicating that the pinning-down phenomenon exists and the measurement frequency is too fast for the ferroelectric domains to rotate with the electric field.

Detailed room-temperature P–E hysteresis loops of the oxide-doped PFSN ceramics are shown in Fig. 3. Both the MnO_2- and Li_2CO_3-doped PFSN ceramics exhibit fully developed, symmetric and saturated P–E hysteresis loops. The hysteresis loops are sharp and narrow accompanied by small value of E_C, which is similar to that of rhombohedral perovskite structure ferroelectrics. Based on the fully saturated P–E hysteresis loops, ferroelectric properties P_r and E_C can be determined, which are shown in Fig. 3. As compared to the MnO_2-doped PFSN ceramics, the Li_2CO_3-doped

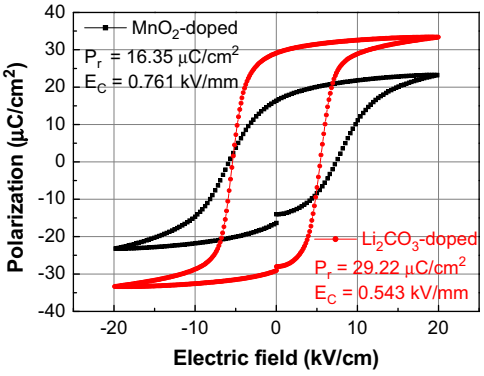

Fig. 3. Room-temperature P–E hysteresis loops of the oxide-doped PFSN ceramics measured at 1 Hz and 2 kV/mm.

PFSN ceramics exhibit large value of P_r and small value of E_C, being 29.22 μC/cm^2 and 0.543 kV/mm, respectively, which is considered as correlating with different charge compensation mechanism induced by oxide doping [22].

Fig. 4 shows room-temperature 3-D graph of relative dielectric constant-frequency-DC bias voltage of the oxide-doped PFSN ceramics. The dielectric response peaks appearing at different frequencies can be attributed to the different vibration modes of electromechanical coupling of the poled ceramics. The dielectric response character is influenced greatly by oxide doping, in which the value of dielectric constant and the shape of dielectric resonant response spectra exhibit great differences. DC bias electric voltage also influences the dielectric response character apparently, which is considered as relating to the electric field induced micro-macro ferroelectric domain change and/or the structural ferroelectric phase transition. Usually, such mechanism can be confirmed by the dielectric-temperature spectrum measurement using the poled ceramics. After poling, an additional dielectric peak or shoulder will be induced, which is considered as correlating with the orientation of ferroelectric domain or the macro-micro domain change upon heating [21]. However, for the oxide-doped PFSN ceramics, the additional electric field-induced minor dielectric peak or shoulder may move to cryogenic temperature, which cannot be measured by our experimental.

For piezoelectric applications the electromechanical coupling coefficient is an important parameter for piezoelectric materials. Frequency dependence of impedance and phase degree of the MnO_2-doped PFSN ceramics is shown in Fig. 5. The MnO_2-doped PFSN ceramics exhibit perfect resonant response peak, which provides efficient energy conversion between electrical energy and mechanical energy. The electromechanical coupling coefficient K_p and the mechanical equality factor Q_m of the MnO_2-doped PFSN ceramics can be calculated from the equations $K_p \approx \sqrt{\frac{f_p - f_s}{f_s} \times 2.51}$ and $Q_m = \frac{f_p^2}{2\pi \cdot f_s \cdot C^T \cdot R(f_p^2 - f_s^2)}$, being 0.232 and 203.8, respectively, at room-temperature.

Environmental temperature exerts great influence on piezoelectric properties of the PFSN-based ceramics due to the existence of depolarization phenomenon of piezoelectric

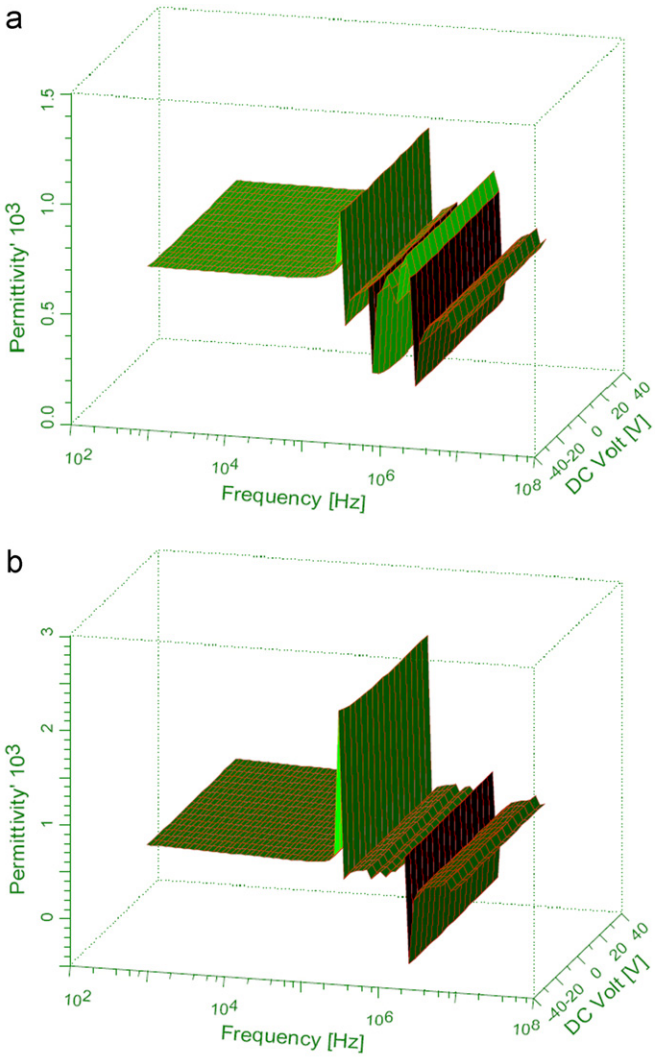

Fig. 4. Frequency dependence of dielectric constant under different DC bias voltage of the poled (a) MnO_2-doped PFSN ceramics and (b) Li_2CO_3-doped PFSN ceramics measured at room-temperature.

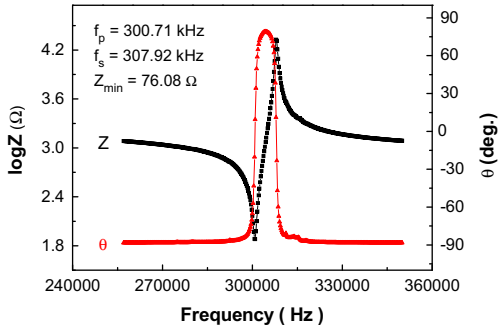

Fig. 5. Frequency dependence of impedance and phase angle degree in radial-extension-vibration-mode of the MnO_2-doped PFSN ceramics measured at room-temperature.

materials. Temperature dependence of radial-extension-vibration electromechanical coupling coefficient K_p and piezoelectric constant d_{33} of the oxide-doped PFSN ceramics is shown in Figs. 6 and 7. These curves can nearly be divided into two regions, in which the values of K_p and d_{33} decrease with different slope upon temperature. The values of K_p and d_{33} decrease slightly from room-temperature to 80 °C, while decrease greatly after 80 °C, till the end of temperature measured. The dramatic decrease of the values of K_p and d_{33} is considered as correlating with the ferroelectric phase transition from rhombohedral ferroelectric phase to cubic paraelectric phase, and can be measured by dielectric property-temperature spectrum. However, the temperature that the values of K_p and d_{33} decreases greatly is rather below than the temperature of the dielectric constant maximum T_m determined by dielectric measurement, which is usually called the depolarization temperature T_d [23]. Therefore, the service temperature is determined based on the experimental results, being around 80 °C, and higher temperature of T_d can be obtained by the addition of $PbTiO_3$ in the PFSN solid solution [9].

Based on the above experimental results and the results reported before, we can draw a conclusion. Oxide doping is an efficient method to improve electrical properties of the PFSN-based ferroelectric ceramics, in which not only the dielectric response peaks become sharp, the dielectric loss decreases, and the dielectric frequency dispersion is suppressed greatly, but also the ferroelectric and piezoelectric properties are improved. Such phenomena can be interpreted

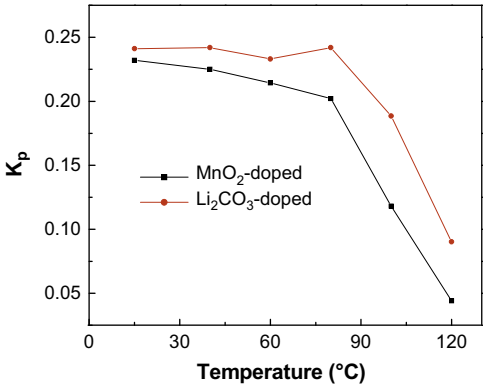

Fig. 6. Temperature dependence of radial electromechanical coupling coefficient K_p of the oxide-doped PFSN ceramics.

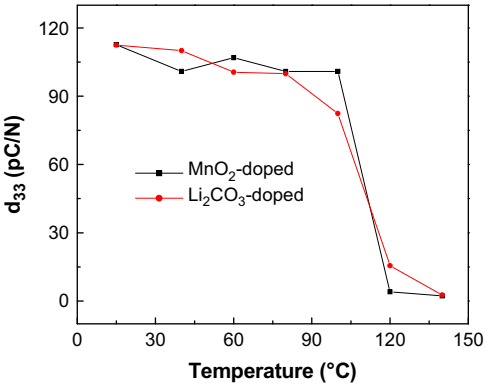

Fig. 7. Temperature dependence of piezoelectric constant d_{33} of the oxide-doped PFSN ceramics.

by a charge compensation mechanism, in which donor defects are generated by manganese ionization $Fe_{Fe}^{x}/Sc_{Sc}^{x}+Mn(3d^5 4s^2)+E_D \rightarrow Mn_{Fe/Sc}^{\cdot}+e'$ and lithium sitting at interstitial sites of the perovskite structure $V_i+Li(2s^1)+E_D \rightarrow Li_i^{\cdot\cdot}+e'$, respectively. Li_2CO_3 doping exhibits enhanced improvement of electrical properties of the PFSN-based ceramics, which can be attributed to the small ionization energy of the interstitial ionic defects, leading to superior compensating for charge disproportion. Therefore, MnO_2 and Li_2CO_3 doping exhibit significant meaning in improving ferroelectric and piezoelectric properties of the PFN- and PSN-based ceramics.

4. Conclusions

Pure rhombohedral perovskite structure oxide-doped PFSN ceramics were prepared by the conventional solid-state reaction method via the B-site oxide mixing route. The oxide-doped PFSN ceramics exhibit large relative density and rather homogenous microstructure morphology. Due to the MnO_2 and Li_2CO_3 doping, the synthesized ceramics exhibit improved dielectric property, and excellent ferroelectric and piezoelectric properties, which are considered as relating to the charge compensation mechanism where donor defects are produced by different ionization paths. The values of P_r and E_C of the MnO_2- and Li_2CO_3-doped PFSN ceramics are 16.35 μC/cm^2 and 0.761 kV/mm, and 29.22 μC/cm^2 and 0.543 kV/mm, respectively. The values of K_p, Q_m and d_{33} of the MnO_2- and Li_2CO_3-doped PFSN ceramics are 0.232, 203.8 and 112.7 pC/N, and 0.241, 320.7 and 112.5 pC/N, respectively. The values of K_p and d_{33} decrease greatly after 80 °C, which is considered as correlating with the ferroelectric phase transition from rhombohedral ferroelectric phase to cubic paraelectric phase. Therefore, oxide doping is an efficient method to improve dielectric, ferroelectric and piezoelectric properties of the PFSN-based ferroelectric ceramics.

Acknowledgments

The authors thank the Qing Lan Project, the Key Laboratory of Inorganic Function Material and Device, Chinese Academy of Sciences (KLIFMD-2011–02) and the Priority Academic Program Development of Jiangsu Higher Education Institutions for financial support.

References

[1] T.R. Shrout, A. Halliyal, Preparation of lead-based ferroelectric relaxors for capacitors, American Ceramic Society Bulletin 66 (1987) 704.
[2] Y.H. Bing, Z.G. Ye, Synthesis and characterizations of the (1-x)Pb($Sc_{1/2}Nb_{1/2}$)O_3-xPbTiO_3 solid solution ceramics, Journal of Electroceramics 21 (2008) 761.
[3] D. Lin, Z. Li, Z.-Y. Cheng, Z. Xu, X. Yao, Electric-field-induced polarization fatigue of [001]-oriented Pb($Mg_{1/3}Nb_{2/3}$)O_3-0.32PbTiO_3 single crystals, Solid State Communications 151 (2011) 1188.
[4] R. Grigalaitis, J. Banys, J. Macutkevic, R. Adomavicius, A. Krotkus, K. Bormanis, A. Sternberg, Broadband dielectric spectroscopy of $PbMg_{1/3}Nb_{2/3}O_3$-$PbSc_{1/2}Nb_{1/2}O_3$ ceramics, Journal of the European Ceramic Society 30 (2010) 613.
[5] H. Uršič, J. Tellier, J. Holc, S. Drnovšek, M. Kosec, Structural and electrical properties of 0.57PSN-0.43PT ceramics prepared by mechanochemical synthesis and sintered at low temperature, Journal of the European Ceramic Society 32 (2012) 449.
[6] Y.-C. Liou, C.-Y. Shih, C.-H. Yu, Pb($Fe_{1/2}Nb_{1/2}$)O_3 perovskite ceramics produced by simplified wolframite route, Japanese Journal of Applied Physics 41 (2002) 3829.
[7] M. Zhu, C. Chen, J. Tang, Y. Hou, H. Wang, H. Yan, W. Zhang, J. Chen, W. Zhang, Effects of ordering degree on the dielectric and ferroelectric behaviors of relaxor ferroelectric Pb($Sc_{1/2}Nb_{1/2}$)O_3 ceramics, Journal of Applied Physics 103 (2008) 084124.
[8] J.W. Hyun, J. Byun, Y. Kim, G. Kim, Ferroelectric and Dielectric Properties of the Pb($Sc_{1/2}Nb_{1/2}$)O_3 Ceramic System, Journal of the Korean Physical Society 57 (2010) 485.
[9] B. Fang, C. Ding, Q. Du, Y. Shan, K. Tezuka, H. Imoto, Structure and dielectric property of (1-x)Pb($Fe_{1/4}Sc_{1/4}Nb_{1/2}$)O_3-xPbTiO_3 ceramics prepared via a B-site oxide mixing route, Journal of Physics D: Applied Physics 42 (2009) 165408.
[10] D. Viehland, S.J. Jang, L.E. Cross, M. Wuttig, Freezing of the polarization fluctuations in lead magnesium niobate relaxors, Journal of Applied Physics 68 (1990) 2916.
[11] S.-E. Park, S. Wada, L.E. Cross, T.R. Shrout, Crystallographically engineered $BaTiO_3$ single crystals for high-performance piezoelectrics, Journal of Applied Physics 86 (1999) 2746.
[12] K. Uchino, The centennial memorial issue of the ceramic society of Japan, Journal of the Ceramic Society of Japan 99 (1991) 829.
[13] X. Zhao, W. Qu, X. Tan, A.A. Bokov, Z.-G. Ye, Influence of long-range cation order on relaxor properties of doped Pb($Mg_{1/3}Nb_{2/3}$)O_3 ceramics, Physical Review B 79 (2009) 144101.
[14] H. Fu, R.E. Cohen, Polarization rotation mechanism for ultrahigh electromechanical response in single-crystal piezoelectrics, Nature 403 (2000) 281.
[15] Z.-G. Ye, Crystal chemistry and domain structure of relaxor piezocrystals, Current Opinion in Solid State and Materials Science 6 (2002) 35.
[16] R.A. Eichel, Defect structure of oxide ferroelectrics-valence state, site of incorporation, mechanisms of charge compensation and internal bias fields, Journal of Electroceramics 19 (2007) 9.
[17] S.-H. Yoon, C.A. Randall, K.H. Hur, Difference between resistance degradation of fixed valence acceptor (Mg) and variable valence acceptor (Mn)-doped BaTiO3 ceramics, Journal of Applied Physics 108 (2010) 064101.
[18] J.P. Attfield, A cation control of perovskite properties, Crystal Engineering 5 (2002) 427.
[19] W. Liu, G. Wang, S. Cao, C. Mao, C. Yao, F. Cao, X. Dong, The Phase Transition Behavior of (1-x)Pb($Sc_{0.5}Ta_{0.5}$)O_3-(x)PbHfO_3 Ceramics, Journal of the American Ceramic Society 94 (2011) 2530.
[20] B. Fang, R. Sun, Y. Shan, K. Tezuka, H. Imoto, On the feasibility of synthesizing complex perovskite ferroelectric ceramics via a B-site oxide mixing route, Journal of Materials Science 42 (2007) 9227.
[21] B. Fang, K. Qian, F. Miao, N. Yuan, J. Ding, X. Zhao, H. Xu, H. Luo, Structural, optical and improved electrical properties of relaxor-based single crystals after poling, Journal of the American Ceramic Society 95 (2012) 1949.
[22] B. Fang, Y. Shan, K. Tezuka, H. Imoto, Improvement of dielectric properties in iron-contained ferroelectrics, Japanese Journal of Applied Physics 44 (2005) 5030.
[23] R. Sun, X. Zhao, Q. Zhang, B. Fang, H. Zhang, X. Li, D. Lin, S. Wang, H. Luo, Growth and orientation dependence of electrical properties of 0.92$Na_{0.5}Bi_{0.5}TiO_3$-0.08$K_{0.5}Bi_{0.5}TiO_3$ lead-free piezoelectric single crystal, Journal of Applied Physics 109 (2011) 124113.